Modified MHC Class II–Associated Invariant Chain Induces Increased Antibody Responses against *Plasmodium falciparum* Antigens after Adenoviral Vaccination

Cyrielle Fougeroux,* Louise Turner,* Anders Miki Bojesen,† Thomas Lavstsen,* and Peter Johannes Holst*

Adenoviral vectors can induce T and B cell immune responses to Ags encoded in the recombinant vector. The MHC class II invariant chain (Ii) has been used as an adjuvant to enhance T cell responses to tethered Ag encoded in adenoviral vectors. In this study, we modified the Ii adjuvant by insertion of a furin recognition site (Ii-fur) to obtain a secreted version of the Ii. To test the capacity of this adjuvant to enhance immune responses, we recombined vectors to encode *Plasmodium falciparum* virulence factors: two cysteine-rich interdomain regions (CIDR) α1 (*IT4var19* and *PFCLINvar30 var* genes), expressed as a dimeric Ag. These domains are members of a highly polymorphic protein family involved in the vascular sequestration and immune evasion of parasites in malaria. The Ii-fur molecule directed secretion of both Ags in African green monkey cells and functioned as an adjuvant for MHC class I and II presentation in T cell hybridomas. In mice, the Ii-fur adjuvant induced a similar T cell response, as previously demonstrated with Ii, accelerated and enhanced the specific Ab response against both CIDR Ags, with an increased binding capacity to the cognate endothelial protein C receptor, and enhanced the breadth of the response toward different CIDRs. We also demonstrate that the endosomal sorting signal, secretion, and the C-terminal part of Ii were needed for the full adjuvant effect for Ab responses. We conclude that engineered secretion of Ii adjuvant–tethered Ags establishes a single adjuvant and delivery vehicle platform for potent T and B cell–dependent immunity. ***The Journal of Immunology*****, 2019, 202: 2320–2331.**

Adenoviruses are a promising solution for a new generation of vaccines to replace vaccines that are either financially and/or technically challenging to generate (1–3) (also see the U.S. National Library of Medicine website, https://clinicaltrials.gov/ct2/results?cond=&term=adenovirus&cntry=&state=&city=&dist, to review the diverse array of existing adenovirus clinical trials). Indeed, adenoviruses are robust vehicles for transient gene delivery (4, 5) and elicit potent and long-lasting transgene-targeted immune responses (6–9). However, whereas the viral capsid provides extracellular Ags for induction of $CD4^+$ T cell responses, the transgene is delivered solely in the adenoviral DNA. Accordingly, the encoded Ag is preferentially presented to the immune system through MHC class I (MHCI), and the transgene-specific T cell response is shown to be mostly $CD8^+$ T cell–mediated (10). Conversely, studies have shown that Abs play a primary role in protection after vaccination (11–13), and $CD4^+$ helper T cells are required after viral infection to stimulate B cells to proliferate, affinity maturate, and secrete Abs for weeks after immunization (14–16). Therefore, to obtain potent and long-lasting transgene immunity after vaccination with adenovirus, concomitant helper T cells and B cell priming against the transgene might be needed to improve Ab responses.

To increase the transgene immune response after adenoviral vaccination, different methods have proven efficient, such as engineering the Ag for secretion (17), oligomerization (18), or increased transgene expression (19). Currently, one of the best genetic adjuvants is fusion of Ags to the C terminus of the MHC class II (MHCII)-associated invariant chain (Ii), which was shown to increase both MHCII and MHCI presentation, inducing higher T cell responses in mice (20, 21) and in primates (22, 23) after adenoviral vaccination. Enhancement of MHCI presentation is not yet fully understood (24); however, MHCII presentation is increased as a result of Ii being a direct transporter of the Ag to the MHCII loading compartment (direct pathway) (25–28). Additionally, tethering of the transgene to the Ii also enables the transport of the Ii–Ag for direct presentation on the cell surface of all infected cells. Therefore, the presence of the complex on the cell surface allows direct presentation of the Ag as well as reuptake into the endosomes (indirect pathway), thanks to the endosomal sorting signal (ESS) domain (29–32). However, the Ii has been shown to induce a limited increase in humoral responses, and therefore we hypothesized that further secretion of an Ii–Ag complex

*Center for Medical Parasitology, Department of International Health, Immunology and Microbiology, University of Copenhagen, 2200 Copenhagen, Denmark; and †Department of Veterinary and Animal Sciences, University of Copenhagen, 1870 Frederiksberg, Denmark

ORCID: 0000-0002-7566-8377 (C.F.).

Received for publication September 4, 2018. Accepted for publication February 1, 2019.

This work was supported by the Center for Research in Pig Production and Health, the University of Copenhagen Research Centre for Control of Antibiotic Resistance, Axel Muusfeldts, Sirion Biotech, the Torben og Alice Frimodts Fond, the Novo Nordisk Foundation (NNF16OC0023362), the Danish Council for Independent Research, and the Sapere Aude program (DFF–4004-00624B).

Address correspondence and reprint requests to Dr. Cyrielle Fougeroux, University of Copenhagen, Center for Medical Parasitology, Blegdamsvej 3B, Bygning 07-11, 2200 København N, Denmark. E-mail address: cyrielle@sund.ku.dk

The online version of this article contains supplemental material.

Abbreviations used in this article: AUC, area under the curve; avg., average; CIDR, cysteine-rich interdomain region; EPCR, endothelial protein C receptor; ESS, endosomal sorting signal; fur, furin recognition site; hAd5, human adenovirus type 5; huCMV, human CMV promoter; IFU, infectious unit; Ii, invariant chain; Ii-Ctermfur, Ii with a C-terminal furin cleavage; Ii-fur, Ii adjuvant by insertion of a fur; Δ17-Ii-fur, Ii deleted in the first 17 aa inserted with the furin site; MHCI, MHC class I; MHCII, MHC class II; MOI, multiplicity of infection; PfEMP1, *P. falciparum* erythrocyte membrane protein 1; rhEPCR, recombinant human EPCR; SN, supernatant; Sp-alb, albumin signal peptide; TGN, trans-Golgi network; WT, wild-type.

would increase B cell immune responses while potentially maintaining the T cell adjuvant effect shown with the native Ii sequence.

To test this, we designed a strategy in which a synthetic furin recognition site (fur) was inserted between the CLIP and the trimerization domain of the Ii sequence and upstream of the C-terminal trimerization domain (33) to direct secretion of a trimerized Ag. The Ag thus secreted would become tethered to the C terminus of the Ii, which was considered beneficial, primarily to ensure oligomerization, but it would also link it to the C-terminal part of the Ii that, in soluble form, inhibits immune signaling pathways implicated in parasite immune evasion (34, 35). Furin is an endoprotease that is mostly active in the trans-Golgi network (TGN), where it cleaves preproteins containing the following recognition site: Arg–X–Lys/Arg–Arg in the secretory pathway (36). From predictions, cleavage of an Ii–Ag complex in the TGN would therefore sort the Ag to the plasma membrane for secretion to the extracellular compartment, as shown in Fig. 1, thereby increasing Ag accessibility to B cells. As Ii also exhibits TGN-independent sorting to endosomes, with the ESS and a direct capacity to enhance MHCI loading, the result might be a concomitant increase in Ag presentation to $CD4^+$ T cells, $CD8^+$ T cells, and B cells.

To test the ability of the proposed adjuvant to increase immune responses, we used known *Plasmodium falciparum* virulence-associated proteins as model Ags. *P. falciparum* is the causative agent of most clinical cases of malaria, one of the most lethal infectious diseases worldwide (37). *P. falciparum* malaria pathogenesis is due to parasite sequestration in the host organs, mediated by *P. falciparum* erythrocyte membrane protein 1 (PfEMP1) binding to endothelial protein C receptor (EPCR) (38, 39). Immunity to severe malaria is thought to be mediated through Abs targeting the EPCR-binding cysteine-rich interdomain region (CIDR) α1 domains, which in response to immune-mediated selection have diversified in sequence but retained a common structure for EPCR binding (40). We chose to work with two CIDRα1.1 domain variants, CIDRα1.1_IT4var19 and CIDRα1.1_PFCLINvar30, in the anticipation that oligomeric immunogens may eventually be a requirement for vaccination against many of the main vaccine challenges (e.g., malaria, HIV, and cancer).

This paper describes the immunogenic properties of our newly designed adjuvant, Ii adjuvant by insertion of a fur (Ii-fur), by detecting immune responses to the fused CIDRα1.1 Ags in adenoviral vaccine, as well as to a panel of recombinant CIDRα1 protein variants. We show that CIDRα1.1 Ags with N- and C-terminal extensions are secreted through the Ii-fur adjuvant and preserve their natural conformation. When expressing Ii-fur–linked CIDRα1.1 domains, we showed that the insertion of a fur promoted Ag secretion while retaining Ii adjuvant capacities. Additionally, in vivo, the Ii-fur tethering of the Ag was capable of inducing an increased CIDRα1 Ab response compared with Ags fused to Ii alone but was dependent on the ESS and the C-terminal domain of the Ii to obtain the full adjuvant effect. We conclude that the Ii adjuvant, with the fur allowing secretion of the tethered Ag to Ii, is an efficient adjuvant system to induce both improved T and B cell responses after adenoviral vaccination.

Materials and Methods

Ethical statements

Female BALB/c mice at the age of 6–8 wk were purchased from Taconic M&B (Ry, Denmark) and housed at the Panum Institute (Copenhagen, Denmark). All experiments were initiated after allowing the mice to acclimatize for at least 1 wk. Experiments were approved by the National Animal Experiments Inspectorate (Dyreforsøgstilsynet, license no. 2011/561-120) and performed according to national guidelines.

Design and production of adenoviral vaccines

Different adenoviral constructs were designed based on replication-deficient *E1*-deleted human adenovirus type 5 (hAd5) (41), in which all adjuvant–Ag complexes were inserted in the *E1* region. The encoded Ags were fused to the C terminus of five different adjuvants: albumin signal peptide (Sp-alb), Ii, Ii-fur, Ii deleted in the first 17 aa inserted with the furin site (Δ17-Ii-fur), and Ii with a C-terminal furin cleavage (Ii-Cterm-fur) (Fig. 2). For MHCI- and II-restricted Ag presentation studies, the same constructs were engineered to encode chicken OVA with its endogenous stop site (Fig. 2A), except for the secreted form of OVA, corresponding to the Sp-alb for the CIDRα1.1, in which no signal peptide was inserted as OVA already contains one for secretion. For immunogenicity studies, the adenovirus constructs were inserted with CIDRα1.1 of *pfemp1* genes

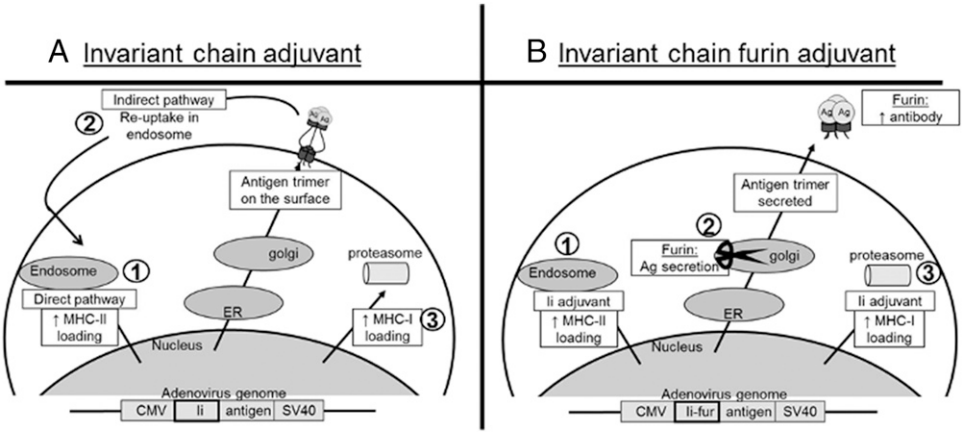

FIGURE 1. Schematic theories of the intracellular mechanism and function of Ii and Ii-fur. (**A**) 1) After adenoviral infection, the Ii–Ag trimer (because of the Ii trimerization domain) is either transported to the endosomes through the ESS (1–17 first peptides), where the Ii–Ag complex will be degraded due to low pH. The presence of the complex in the endosomes increases the chances of the fused Ag peptides to be presented on MHCII and, therefore, enhances the $CD4^+$ response to the Ag. This is called direct presentation. 2) The indirect presentation is due to the fact that Ii–Ag complex is also sorted to the TGN and will be presented on the surface of the cell, where it will be available for reuptake in the endosomes thanks to the ESS and follow the same route as the direct pathway from there. 3) Ii also increases MHCI presentation; however, the mechanism is not yet known. (**B**) After infection of the cells with the adenovirus inserted with Ii-fur adjuvant, as seen with the Ii, it can be transported either directly to the endosomes or through the TGN. 1) If it is directly transported to the endosomes, the direct pathway for increased MHCII should be conserved. 2) However, when the Ii is transported to the Golgi, the furin protease will be active and cleave the fur inserted in the complex prior to the trimerization domain. A cleaved protein in the Golgi will be sorted to the plasma membrane for secretion, and therefore a trimerized Ag fused to a part of Ii will be transported to the extracellular compartment to be secreted out of the cell. This will increase the accessibility of our Ag to both $CD4^+$ T cells and B cells while retaining partly MHCII loading enhancement through the direct pathway and 3) similar to the Ii adjuvant, potential MHCI loading enhancement.

A

name	sequence (promoter ← Ii or modified Ii → antigen PolyA)	Endosomal sorting signal (ESS)	trimerisation	secretion
Ii-fur-OVA	CMV ESS TM domain CLIP Furin Trimerisation domain OVA SV40	X	X	X (trimer)
Ii-OVA	CMV ESS TM domain CLIP Trimerisation domain OVA SV40	X	X	
Δ17-Ii-fur-OVA	CMV TM domain CLIP Furin Trimerisation domain OVA SV40		X	X (trimer)
Ii-Cterm-fur-OVA	CMV ESS TM domain CLIP Trimerisation domain Furin OVA SV40	X	X	X (monomer)
OVA	CMV OVA SV40			X (monomer

B

name	sequence (promoter ← Ii or modified Ii → ← antigens → PolyA)	Endosomal sorting signal (ESS)	trimerisation	secretion
Ii-fur-19-30	CMV ESS TM domain CLIP Furin Trimerisation domain IT4var19 PFCLINvar30 SV40	X	X	X (trimer)
Ii-19-30	CMV ESS TM domain CLIP Trimerisation domain IT4var19 PFCLINvar30 SV40	X	X	
Δ17-Ii-fur-19-30	CMV TM domain CLIP Furin Trimerisation domain IT4var19 PFCLINvar30 SV40		X	X (trimer)
Ii-Cterm-fur-19-30	CMV ESS TM domain CLIP Trimerisation domain Furin IT4var19 PFCLINvar30 SV40	X	X	X (monomer)
SP-alb-19-30	CMV IT4var19 PFCLINvar30 SV40			X (monomer

C

FIGURE 2. Sketch of the different hAd5 constructs used in the study. (**A**) Five hAd5 vectors were designed, all encoding chicken OVA fused to different adjuvants (Ii-fur, Ii, Ii-Cterm-fur, and Δ17-Ii-fur) and the standard chicken OVA secreted with the internal signal peptide (OVA). The inserted adjuvant–Ag complexes were flanked by the huCMV and an SV40 polyadenylation signal. (**B**) Five hAd5 vectors were designed encoding dimeric Ags: IT4var19 and PFCLINvar30 CIDRα1.1 domains fused to different adjuvants (Ii-fur, Ii, Sp-alb, Ii-Cterm-fur, and Δ17-Ii-fur). The inserted adjuvant–Ag complexes were flanked by the huCMV and an SV40 polyadenylation signal. (**C**) Schematic representation of the Ags produced with the different adenovirus constructs. Ii-fur and Δ17-Ii-fur will secrete a trimeric Ag and Ii-Cterm-fur and Sp-alb adjuvants will produce a secreted monomer, whereas Ii will have a trimeric Ag–Ii complex bound to the surface of the cell.

IT4var19 and *PFCLINvar30* linked by a G-S linker (referred to as "19–30" in figures) and expressed as they would be in a polymeric vaccine by removing the stop codon and using a downstream codon to add a C-terminal tail (Fig. 2B). The inserted adjuvant–Ag complexes were flanked by the human CMV promoter (huCMV) and an SV40 polyadenylation signal. For all constructs, hAd5 vectors were produced by homologous recombination in BJ5183 cells (42). In vitro expression of the encoded Ags was placed under the control of a tetracycline operator (43). After amplification in HEK293 cells expressing a tetracycline repressor, the adenoviruses were purified using a caesium chloride gradient as described elsewhere (44).

Ag identification and secretion

Production and purification of recombinant Ags used for immunoassays (recombinant CIDRα1 and recombinant human EPCR [rhEPCR]) were produced internally as explained by Turner et al. (45). Secretion of the Ags was investigated by infecting COS7 cells with 10 infectious units (IFU)/cell or VERO cells with 50 IFU/cell with the different hAd5 constructs inserted with CIDRα1.1 IT4var19–PFCLINvar30. After 24 h, incubation medium was replaced with serum-free medium. Supernatant (SN) and cells were harvested 48 h postinfection, and cells were lysed with NP40 (Invitrogen) and protease inhibitor mixture. SN was concentrated using Vivaspin 20 columns (Sartorius). SN from infected cells were run on SDS-PAGE and recognized by immunized rat serum against the two encoded CIDRα1.1 proteins. The primary Ab was recognized with an anti-rat alkaline phosphatase Ab (Calbiochem) revealed with BCIP/NBT tablets (Sigma-Aldrich). Quantification of the Western blot was done by ImageQuant TL, in which the number of pixels for each band was detected thanks to similar-size squares. Functionality of IT4var19 and PFCLINvar30 CIDRα1.1 protein domains in SN and cell lysates of COS7 cells was investigated by testing the binding to their natural ligand, human EPCR. After coating Nunc MaxiSorp plates with 3 μg/ml rhEPCR ectodomain, SN and cell lysates were added to the wells. Interaction of the two proteins was revealed by recognition of either anti-CIDRα1.1_IT4var19 or anti-CIDRα1.1_PFLCINvar30 rat sera. Rat Abs were recognized with HRP-conjugated polyclonal rabbit anti-rat (Invitrogen). OD was measured at 450 nm using an ELISA plate reader (VersaMax; Molecular Devices). To further investigate the functionality of IT4var19 and PFCLINvar30 CIDRα1.1 protein domains in SN, adenovirus SN from COS7 cells infected with Ii-fur–IT4var19–PFLCINvar30 or recombinant PfEMP1 protein (HB3var03) was panned on rhEPCR-coated wells (3 μg/ml). The procedure was repeated four times to ensure complete depletion. Fifty microliters of the EPCR-depleted and nondepleted SN or 5 μg/ml of the EPCR-depleted and nondepleted proteins were used to coat ELISA plates. After blocking, rat polyclonal anti-CIDRα1.1_IT4var19 or anti-CIDRα1.1_HB3var03 serum was added to the wells. Proteins were identified with anti-rat HRP and revealed using TMB PLUS (Kem-En-Tec Diagnostics). OD was measured at 450 nm using an ELISA plate reader (VersaMax; Molecular Devices).

Analyses of MHCI and MHCII presentation of OVA

For MHCI Ag presentation, JAWSII cells were infected with 250 multiplicity of infection (MOI)/cell of the different hAd5 constructs inserted with OVA (Fig. 2A). The next day, cells were washed and stained with anti-mouse H-2K^b bound to SIINFEKL-PE (BioLegend). Fluorescence was analyzed on a FACSCalibur (BD Biosciences). For MHCII Ag presentation, 10^5 JAWS cells were infected with 250 MOI/cell of the different hAd5 constructs inserted with OVA (Fig. 2A). Twenty-four hours later, cells were washed and incubated with 4×10^4 BO-97.10 cells, T cell hybridomas that respond to a chicken OVA peptide (aa 327–339) bound to MHCII, a generous gift from J. Kappler and P. Marrack (46). After 96 h of coculture, SN was harvested, and Il-2 levels were measured by ELISA (eBioscience).

Analyses of T cell responses

To measure specific T cell responses, BALB/C mice were vaccinated in the right hind paw with 2×10^6 IFU of hAd5–Ii-fur–IT4var19–PFCLINvar30 ($n = 5$), hAd5–Sp-alb– IT4var19–PFCLINvar30 ($n = 5$), or hAd5–Ii-IT4var19–PFCLINvar30 ($n = 5$). Seven days later, the spleens were harvested, and lymphocytes were incubated with relevant peptides (1 μg/ml PFCLINvar30$^{182-190}$) at 37°C and 5% CO_2 for 5 h. After incubation, cells were stained according to standard protocols as described by Ragonnaud et al. (47) using the following Abs (BioLegend): CD8_PerCP.Cy5.5,

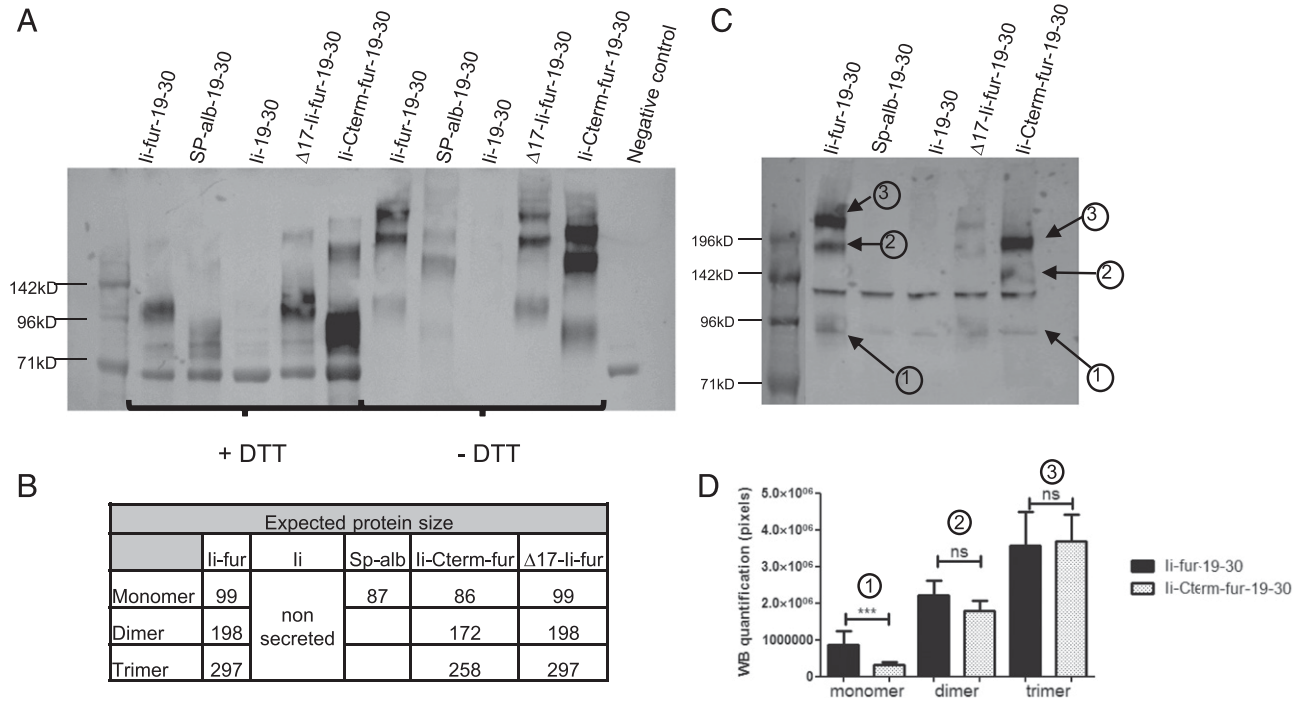

Expected protein size					
	Ii-fur	Ii	Sp-alb	Ii-Cterm-fur	Δ17-Ii-fur
Monomer	99	non secreted	87	86	99
Dimer	198			172	198
Trimer	297			258	297

FIGURE 3. The proteins encoded with Ii-fur adjuvant are secreted as trimers. (**A**) Identification of CIDRα1.1_PFCLINvar30 by Western blot in denaturing (+DTT) and nondenaturing conditions (−DTT) in the SN of infected VERO cells with 50 IFU/cell of hAd5–Ii-fur–IT4var19–PFCLINvar30, hAd5–Sp-alb–IT4var19–PFCLINvar30, hAd5–Ii–IT4var19–PFCLINvar30, hAd5–Δ17-Ii-fur–IT4var19–PFCLINvar30, or hAd5–Ii-Cterm-fur–IT4var19–PFCLINvar30 virus. (**B**) Explanatory table showing the expected migration band size of the above secreted proteins. (**C**) Identification of CIDRα1.1_PFCLINvar30 by Western blot in nondenaturing conditions (−DTT) in the SN of infected COS7 cells with 50 IFU/cell of hAd5–Ii-fur–IT4var19–PFCLINvar30, hAd5–Sp-alb–IT4var19–PFCLINvar30, hAd5–Ii–IT4var19–PFCLINvar30, hAd5–Δ17-Ii-fur–IT4var19–PFCLINvar30, or hAd5–Ii-Cterm-fur–IT4var19–PFCLINvar30 virus for quantification analysis. (**D**) Quantification analysis of the bands present on the Western blot for hAd5–Ii-fur–IT4var19–PFCLINvar30 and hAd5–Ii-Cterm-fur–IT4var19–PFCLINvar30 virus secreted in infected COS7 cells. The above Western blot shows the analyzed bands: 1 for monomer, 2 for dimer, and 3 for trimer. Several Western blots from the same infected cells were quantified; each bar represents the mean of the triplicates, and the number of pixels was compared between the two viruses with nonparametric Mann–Whitney *U* tests. ***$p < 0.0001$. ns, not significant.

CD4_FITC, B220_Pacific Blue, CD44_allophycocyanin, IFN-γ_allophycocyanin, and TNF-α_PeCy7. The data were collected on a Fortessa 3-laser instrument (BD Biosciences) and analyzed using FlowJo software (Tree Star, Ashland, OR).

Vaccination in mice for assessment of Ab responses

Female BALB/c or C57BL/6 mice were vaccinated on day 0 with 2×10^9 particles i.m. with hAd5–Ii-fur–IT4var19–PFCLINvar30, hAd5–Sp-alb–IT4var19–PFCLINvar30, hAd5–Ii–IT4var19–PFCLINvar30, hAd5–Δ17-Ii-fur–IT4var19–PFCLINvar30, or hAd5–Ii-Cterm-fur–IT4var19–PFCLINvar30 ($n = 5$ per group) and boosted 8 wk later with a homologous boost (2×10^9 particles i.m.). Blood samples were harvested prior to vaccination to use as an internal control, as well as 2, 6, and 10 wk after the first vaccination.

Detection of Abs by ELISA

Nunc MaxiSorp plates were coated with 5 μg/ml IT4var19 or PFCLINvar30 recombinant CIDRα1.1 protein domain, produced as previously described (40). When comparing Ii-fur to Sp-alb and Ii, vaccine serum was diluted to 1:50 and analyzed at a single dilution (week 2 and week 6) or in 3-fold dilutions (week 10). To compare between all the mutants, serum was diluted to 1:5 and analyzed at a single dilution (week 2 and week 6) or in 2-fold dilutions (week 10), based on previous optimization. Abs recognizing specifically CIDRα1.1_IT4var19 or CIDRα1.1_PFCLINvar30 were detected with HRP-conjugated polyclonal rabbit anti-mouse Ig (P260; DAKO, Glostrup, Denmark). The presence of Abs was detected using TMB PLUS (Kem-En-Tec Diagnostics). OD was measured at 450 nm using an ELISA plate reader (VersaMax; Molecular Devices) (48).

Detection of inhibitory Abs by ELISA

To test the capacity of the induced Abs to inhibit binding of the encoded Ags to their natural ligand (EPCR), Nunc MaxiSorp plates were coated with 3 μg/ml rhEPCR. Mouse serum, diluted to 1:50, was mixed with recombinant IT4var19 or PFCLINvar30 proteins, tagged with V5, and tested for the ability of the Ab to prevent the recombinant proteins from binding to EPCR. Binding to EPCR was identified by HRP Ig anti-V5 tag and revealed using TMB PLUS (Kem-En-Tec Diagnostics). OD was measured at 450 nm using an ELISA plate reader (VersaMax; Molecular Devices).

Analyses of cross-reactive Abs by Luminex

Cross-reactive Abs were detected in serum of BALB/c mice 10 wk after vaccination using multiplex assay. In brief, serum was diluted to 1:50 and incubated with 45 microsphere beads, each coated with a different CIDRα1 protein variant, thus representing the sequence variation among CIDRα1 domains (40). IgG reactivity to the beads was quantified by luminescence, as described by Cham et al. (45).

Statistical analysis

Nonparametric Mann–Whitney *U* tests were performed for assessing immune responses using Ii-fur adjuvant as compared with the other adjuvants. For recognition ELISA, sera from week 10 were diluted in serial fold dilutions in the wells and analyzed with a nonlinear regression curve. Areas under the curve (AUC) were calculated and plotted for comparison. Statistical analyses were performed using GraphPad Prism, and p values <0.05 were considered significant.

Results

Different genetic adjuvants were inserted into hAd5 vectors to study the properties of the Ii-fur adjuvant (Figs. 1, 2) in the context of two different Ags (OVA for MHC-restricted Ag presentation studies and CIDRα1.1 domains for immunogenicity studies). The

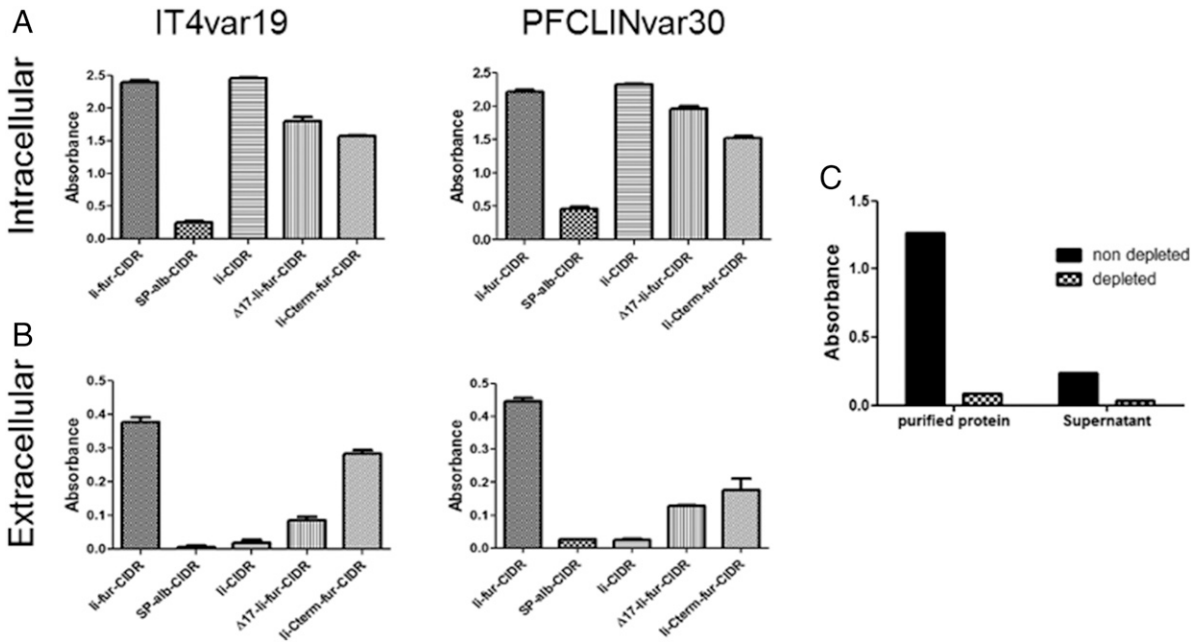

FIGURE 4. The proteins encoded with Ii-fur adjuvant are correctly folded. (**A** and **B**) Analysis of the capacity to bind to EPCR by expressed proteins in the SN (extracellular) or cell lysates (intracellular) after infection of COS7 cells with 10 IFU/cell of hAd5–Ii-fur–IT4var19–PFCLINvar30, hAd5–Sp-alb–IT4var19–PFCLINvar30, hAd5–Ii–IT4var19–PFCLINvar30, hAd5–Δ17-Ii-fur–IT4var19–PFCLINvar30, or hAd5–Ii-Cterm-fur–IT4var19–PFCLINvar30 virus. Each bar represents the mean of the triplicates with SD. (**C**) SN from COS7 cells infected with hAd5–Ii-fur–IT4var19–PFCLINvar30 and HB3var03 purified protein were tested for IT4var19 or HB3var03 Ab recognition in ELISA before (nondepleted) or after (depleted) sequestration of the proteins by EPCR binding. Each bar represents the mean of duplicates done for each condition.

adenovirus 5 containing the Ii-fur adjuvant was compared with a secreted encoded Ag (Sp-alb) and to Ii-tethered Ag, two well-known adjuvants in the literature. To explore the importance of the trimerization domain of the Ii, the fur was inserted after the trimerization domain (Ii-Cterm-fur), thus preventing any Ii-mediated role of the secreted C terminus in Ii attachment to the secreted Ag while keeping the other adjuvant effects of the Ii and secretion. ESS was deleted (Δ17-Ii-fur) from the Ii, as it has been suggested to be important for MHCII presentation (29, 30, 32). This will impair both indirect and direct pathways through the endosomes, thus potentially affecting $CD4^+$ T cell and B cell responses. All constructs and properties of each adjuvant can be seen in Fig. 2.

Analysis of the expression of encoded CIDRα1.1 Ags

To confirm the secretion of the encoded *P. falciparum*–derived Ags (CIDRα1.1_IT4var19 and CIDRα1.1_PFCLINvar30) with the Ii-fur adjuvant, COS7 and VERO cells were infected with the five different hAd5 constructs (Fig. 2B). SN were run on a Western blot under both denaturing (SDS plus DTT) and partially denaturing (SDS minus DTT) conditions. Secretion of the coupled Ags was analyzed from VERO cells (Fig. 3A, 3B) and COS7 cells (Fig. 3C, 3D). Under both denaturing and nondenaturing conditions (Fig. 3A), we could confirm secretion of the proteins from Ii-fur, Sp-alb, Ii-Cterm-fur, and Δ17-Ii-fur constructs, confirming our theory that the insertion of a furin site would induce secretion, as opposed to the Ii construct. Additionally, the constructs with furin inserted internally in the Ii (Ii-fur and Δ17-Ii-fur) induced a secreted protein of higher weight (Fig. 3B) compared with proteins secreted without tethered Ii (Ii-Cterm-fur and Sp-alb). Under nondenaturing conditions (Fig. 3A, 3C), we could detect a trimeric CIDRα1.1_PFCLINvar30 of the expected size in the Ii-fur and Δ17-Ii-fur constructs, indicating the trimerization of the Ags as expected due to the presence of the C-terminal Ii. However, other constructs (Sp-alb and Ii-Cterm-fur) also show some high m.w. proteins (dimer and trimer), which is not expected but could be explained by the multiple cysteines present in the CIDRα1 domains inducing oligomerization. To better characterize potential quantitative differences in dimer and trimer secretion of the C-terminal Ag, we quantified the dominant secreted species of Ii-fur– and Ii-Cterm-fur–secreted proteins from COS7 cell SN. These results clearly indicated that dimers and trimers were the predominant antigenic forms of both Ags, and pixel-based quantitation showed an equal ratio for Ii-fur and Ii-Cterm-fur trimer (Fig. 3C, 3D). Therefore, as Ii-Cterm-fur did not produce a monomeric version of the Ag as expected, this construct will further be used only to determine the role of the C-terminal domain in the Ii-fur adjuvant effect. Similar results were obtained for detection of CIDRα1.1_IT4var19 in VERO cells (data not shown). To investigate if the correct folding and accessibility of the Ags were preserved even with multimerized Ags (Ii-fur, Δ17-Ii-fur, Ii, and Ii-Cterm-fur) and potential aggregation as seen in the Western blot, both cell lysates (Fig. 4A) and SN (Fig. 4B) from COS7 cells were checked for the presence of functional CIDRα1.1 protein. This was done by measuring the ability of the secreted proteins to bind to their natural ligand, EPCR, using the same SN as applied for quantitation in Fig. 3C. We could detect binding to EPCR with both encoded Ags in the SN and cell lysates. Ii-fur constructs (including the mutations Δ17-Ii-fur and Ii-Cterm-fur, albeit to a slightly lesser extent) induced higher levels of EPCR-binding secreted Ags in the SN as compared with Sp-alb. Functional Ii–CIDRα1 Ag was only secreted at minimal levels but retained at high levels intracellularly. These results were expected because Ii-fur constructs Δ17-Ii-fur and Ii-Cterm-fur are secreted through the fur, as opposed to Ii present on the cell membrane. The secretion difference between the Ii constructs and the Sp-alb was also seen when using OVA Ags (data not shown), indicating that Ii might be also used as a chaperone protein intracellularly. These findings confirmed that the conformation of the Ags and accessibility of the EPCR-binding epitopes were not prevented by the

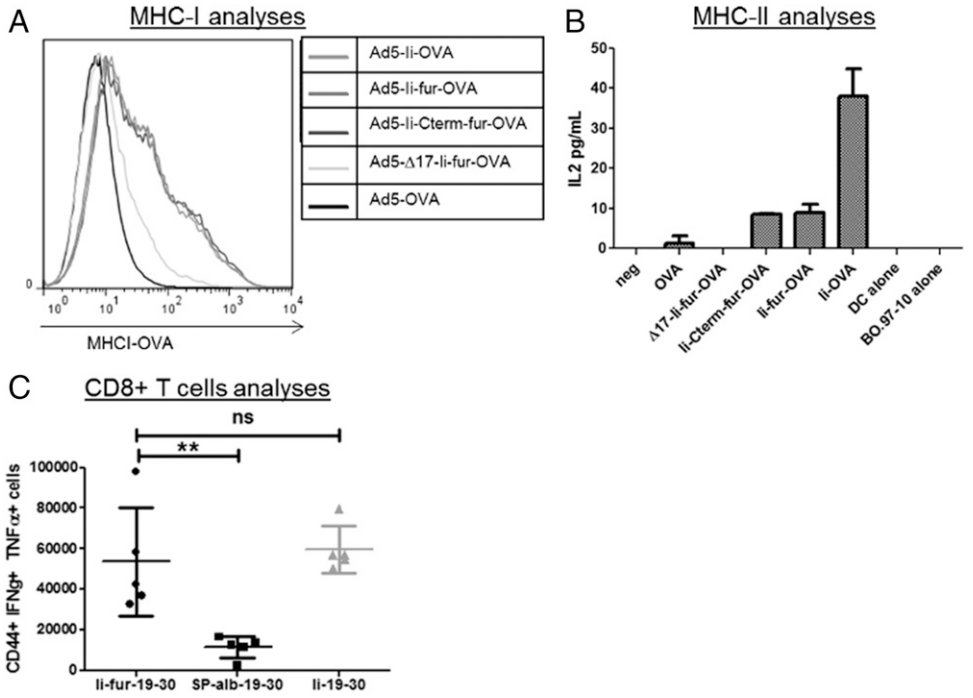

FIGURE 5. The T cell adjuvant effect of the Ii is preserved after insertion of a fur. (**A**) MHCI presentation of OVA on the surface of JAWSII cells after infection with 250 MOI/cell hAd5–Ii-fur–OVA, hAd5–chicken OVA, hAd5–Ii–OVA, hAd5–Δ17-Ii-fur–OVA, or hAd5–Ii-Cterm-fur–OVA virus, analyzed by flow cytometry. (**B**) IL-2 levels representing MHCII presentation of OVA on the surface of JAWSII cells infected with 250 MOI/cell hAd5–Ii-fur–OVA, hAd5–chicken OVA, hAd5–Ii–OVA, hAd5–Δ17-Ii-fur–OVA, or hAd5–Ii-Cterm-fur–OVA virus and recognized by T cells specific for MHCII bound to OVA peptide. Each bar represents the mean of duplicates with SD. (**C**) T cell responses to the encoded Ags from splenocytes 7 d after vaccination of BALB/C mice with hAd5–Ii-fur–IT4var19–PFCLINvar30 ($n = 5$), hAd5–Sp-alb–IT4var19–PFCLINvar30 ($n = 5$), or hAd5–Ii–IT4var19–PFCLINvar30 ($n = 5$) were assessed by flow cytometry after stimulation with the relevant peptide (1 μg/ml PFCLINvar30$^{182-190}$) and surface and intracellular staining. Each group was compared with the Ii-fur adjuvant group with nonparametric Mann–Whitney U tests. $^{**}p < 0.001$. ns, not significant.

trimerization induced by the Ii, which is encouraging for future oligomeric Ag designs. Because we detected some aggregates in the Western blot figures, we further explored the question of how much of the Ag was fully functional, as the potential trimers seen in Ii-fur construct could just be aggregates. As we would not expect aggregates to bind as specifically to EPCR, we subjected the cell SN from Ii-fur–transfected cells to Ag sequestration by EPCR (Fig. 4C). In this experiment, 80% of the secreted Ag was retained by EPCR binding and therefore lost when analyzing the depleted SN. This confirms the specificity of the previous assay and a very high degree of functionally folded EPCR, despite the presence of multiple oligomeric forms. Notably, from these oligomers, we cannot rule out the possibility that only some of the individual EPCR-binding CIDR domains within the oligomers are functional, as this would still lead to EPCR sequestration.

Potency of the Ii-fur adjuvant to retain the T cell adjuvant effect of Ii

In addition to verifying secretion of the Ags, it was important to ensure that the adjuvant effect previously reported for Ii-fused Ags (increase of MHCI and MHCII presentation as well as CD8$^+$ adjuvant) was not altered by the insertion of a fur. To ascertain this, similar constructs to those encoding malaria Ags were made but encoding OVA Ag (Fig. 2A). The insertion of OVA allows direct investigation of MHCI- and MHCII-restricted epitope presentation at the surface of APCs. Dendritic cell–like cells (JAWSII) were infected with the five different OVA adenoviruses and showed a similar increase of MHCI presentation of OVA peptide, with or without the addition of the fur, compared with the construct with secreted OVA (Fig. 5A). However, the Δ17-Ii-fur–OVA-inserted hAd5 showed a decreased presentation of the OVA. This is surprising, as a previous article showed that the endosomal sorting pathway is mainly involved in MHCII presentation and that Δ17-Ii-fur–OVA-inserted hAd5 provides a similar or an improved immune response compared with Ii–OVA-inserted hAd5 (49).

MHCII-restricted Ag presentation was investigated by coculture of dendritic cell–like cells (JAWS II) with T cell hybridomas that specifically respond to a chicken OVA peptide (aa 327–339) bound to MHCII. IL-2 secretion was used as a correlate of activation of CD4$^+$ T cells through MHCII plus OVA peptide as previously described (50). IL-2 levels were higher with the Ii-fur and Ii-Cterm-fur constructs than in the construct without Ii (Fig. 5B), therefore retaining partly the MHCII adjuvant effect of Ii. However, MHCII presentation was lowered in the constructs containing the fur as compared with the nonsecreted wild-type (WT) Ii construct. This was expected, as the secretion of the Ag with the furin cleavage should induce a reduced availability of Ag for endolysosomal proteolysis, impairing reuptake of the Ii through the ESS for processing and presentation of the tethered Ag on MHCII (51), thereby impairing the indirect pathway. The importance of the ESS for the assay was also confirmed by the complete disappearance of MHCII presentation on the surface of the cells with the Δ17-Ii-fur construct, in which the ESS is deleted, thus impairing both the direct and indirect pathways for endosomal sorting necessary for presentation through MHCII (52).

According to these results, the furin insertion did not alter the adjuvant effect of Ii to increase MHCI and MHCII presentation. However, to further confirm that T cell immune responses in vivo were not altered by insertion of the fur, CD8$^+$ T cell responses were assessed by flow cytometry after hind paw vaccination in BALB/c mice. CD8$^+$ T cell responses were shown to be similarly increased when using the Ii and the Ii-fur adjuvant as compared with the

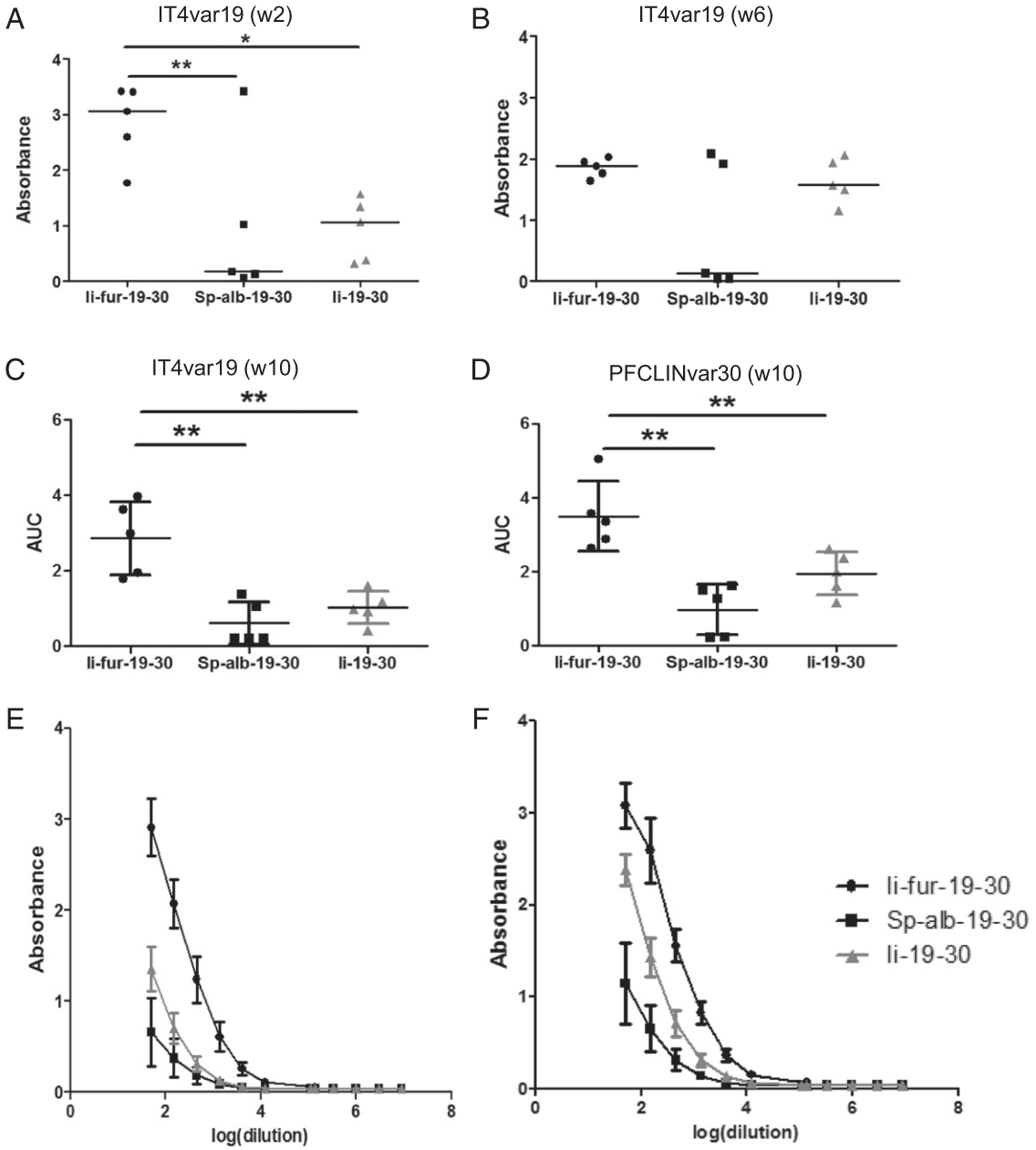

FIGURE 6. Ii-fur adjuvant induces a stronger Ab response toward encoded malaria Ags compared with controls. (**A** and **B**) Detection of Abs recognizing CIDRα1.1_IT4var19 (A) 2 wk or (B) 6 wk after vaccination of BALB/C mice with hAd5–Ii-fur–IT4var19–PFCLINvar30 (n = 5), hAd5–Sp-alb–IT4var19–PFCLINvar30 (n = 5), or hAd5–Ii–IT4var19–PFCLINvar30 (n = 5). Serum was diluted to 1:50. Bars represent the median of each group. (**C** and **E**) Detection of Abs recognizing CIDRα1.1_IT4var19 10 wk after vaccination (2 wk after homologous boost) of BALB/C mice with hAd5–Ii-fur–IT4var19–PFCLINvar30 (n = 5), hAd5–Sp-alb–IT4var19–PFCLINvar30 (n = 5), or hAd5–Ii–IT4var19–PFCLINvar30 (n = 5). Serum was diluted to 1:50 and added to the wells in 3-fold dilutions. (E) Absorbance and dilutions were plotted on a log(x) axis, and AUC were calculated and plotted in (C). Bars represent the mean of each group with the SD. (**D** and **F**) Detection of Abs recognizing CIDRα1.1_PFCLINvar30 10 wk after vaccination (2 wk after homologous boost) of BALB/C mice with hAd5–Ii-fur–IT4var19–PFCLINvar30 (n = 5), hAd5–Sp-alb–IT4var19–PFCLINvar30 (n = 5), or hAd5–Ii–IT4var19–PFCLINvar30 (n = 5). Serum was diluted to 1:50 and added to the wells in 3-fold dilutions. (F) Absorbance and dilutions were plotted on a log(x) axis, and AUC were calculated and plotted in (D). Bars represent the mean of each group with the SD. Each group was compared with the Ii-fur adjuvant group with nonparametric Mann–Whitney U tests. *$p < 0.05$, **$p < 0.001$.

secreted version of the Ag with the Sp-alb (Fig. 5C). These results showed that the overall T cell adjuvant effect of WT Ii was maintained after insertion of the furin cleavage site, and similar results were shown in C57B6 and CB6F1/J mice (data not shown).

Potency of the different adjuvants in inducing Ab responses

The main purpose of inducing secretion of the Ii–Ag complex by inserting a furin cleavage site was to enhance Ab responses to our Ag. Groups of five mice were vaccinated with the different hAd5–CIDRα1.1 constructs (Fig. 2B), and Ab responses were assessed and compared with the Ab responses induced by Ii-fur adjuvant. An enhanced Ab response was detected with the Ii-fur adjuvant as early as 2 wk postvaccination in comparison with secreted Ag (Sp-alb) and WT Ii (Fig. 6A). We noticed that the Ab responses at week 6 show a similar tendency but with lower power (Fig. 6B). However, a significant enhancement of Ab responses with Ii-fur was seen at week 6 when used in a different mouse strain (Supplemental Fig. 1). These results demonstrated that Ii-fur adjuvant triggered an accelerated and enhanced immune response. Ten weeks after first vaccination, which was 2 wk after homologous

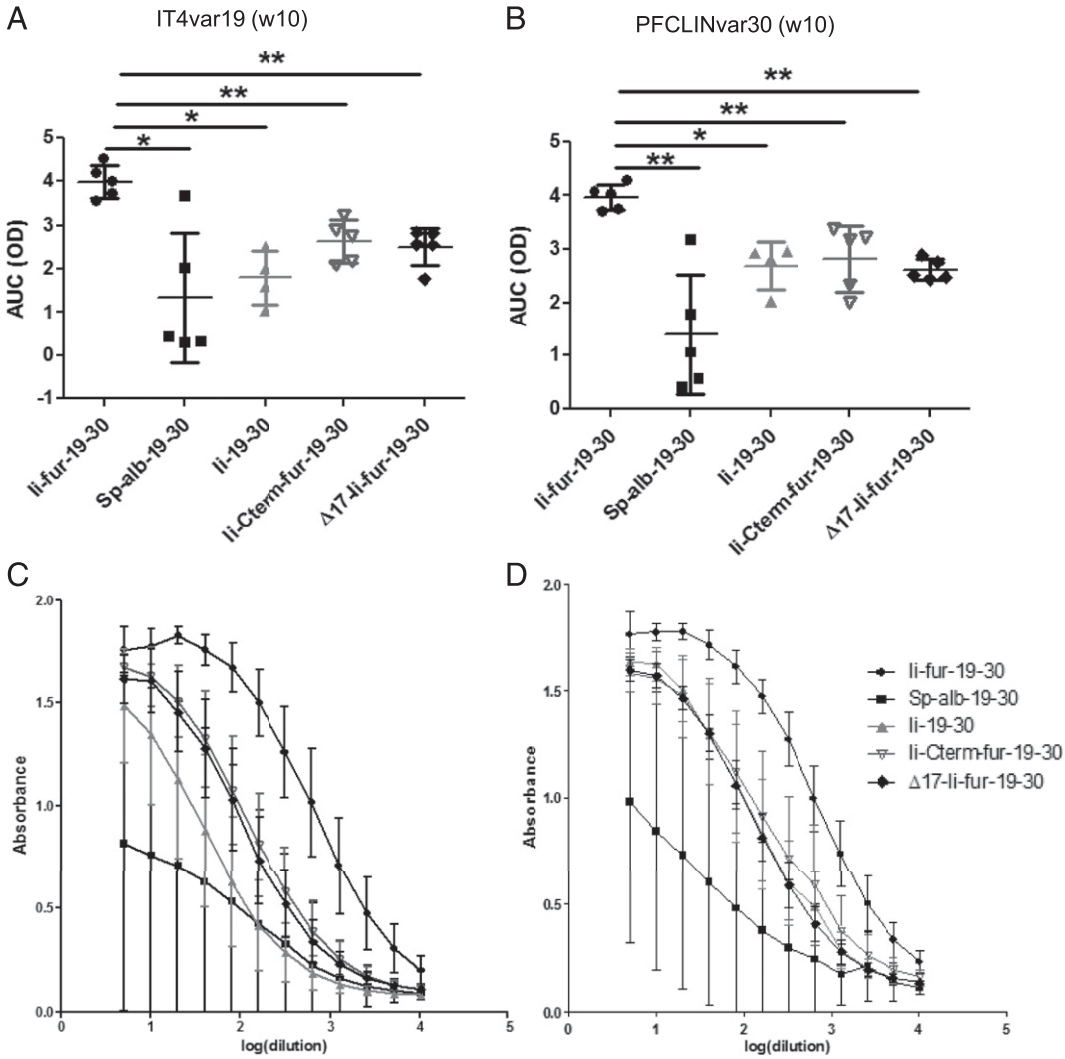

FIGURE 7. ESS and trimerization domains contribute to the adjuvant effect of Ii-fur for Ab responses. (**A** and **C**) Detection of Abs recognizing CIDRα1.1_IT4var19 10 wk after vaccination (2 wk after homologous boost) of BALB/C mice with hAd5–Ii-fur–IT4var19–PFCLINvar30 (n = 5), hAd5–Sp-alb–IT4var19–PFCLINvar30 (n = 5), hAd5–Ii–IT4var19–PFCLINvar30 (n = 4), hAd5–Ii-Cterm-fur–IT4var19–PFCLINvar30 (n = 5), or hAd5–Δ17-Ii-fur–IT4var19–PFCLINvar30 (n = 5). Serum was diluted to 1:5 and added to the wells in 2-fold dilutions. (C) Absorbance and dilutions were plotted on a log(x) axis, and AUC were calculated and plotted in (A). (**B** and **D**) Detection of Abs recognizing CIDRα1.1_PFCLINvar30 10 wk after vaccination (2 wk postboost) of BALB/C mice with hAd5–Ii-fur–IT4var19–PFCLINvar30 (n = 5), hAd5–Sp-alb–IT4var19–PFCLINvar30 (n = 5), hAd5–Ii–IT4var19–PFCLINvar30 (n = 5), hAd5–Ii-Cterm-fur–IT4var19–PFCLINvar30 (n = 5), or hAd5–Δ17-Ii-fur–IT4var19–PFCLINvar30 (n = 5). Serum was diluted to 1:5 and added to the wells in 2-fold dilutions. Absorbance and dilutions were plotted on a log(x) axis (D), and AUC were calculated and plotted in (C). Bars represent the mean of each group with the SD. Each group was compared with the Ii-fur adjuvant group with nonparametric Mann–Whitney U tests. *$p < 0.05$, **$p < 0.001$.

boost injection, the Ab response remained significantly increased after vaccination with the Ii-fur adjuvant in comparison with Ii and Sp-alb constructs for each encoded Ag (Fig. 6C–F). These results showed not only that the Ii-fur adjuvant retained the properties of the endogenous Ii, as discussed previously, but also that the secretion of the Ag enhanced Ab responses after adenoviral vaccination. Similar results were demonstrated with CIDRα1.1 PFCLINvar30 (data not shown) and in the C57BL/6 strain of mice for both Ags (Supplemental Fig. 1).

The role of two different domains of Ii was investigated with the designed mutations (Δ17-Ii-fur and Ii-Cterm-fur) in the enhancement of Ab responses, as compared with the previously used adjuvants (Ii-fur, Ii, and Sp-alb). We found that, even though Δ17-Ii-fur and Ii-Cterm-fur still induced an increased Ab response as compared with Ii and Sp-alb constructs, it was significantly lower than that induced by the full adjuvant Ii-fur (Fig. 7). Therefore, we concluded that the deletion of the ESS sequence and insertion of the fur after the trimerization domain negatively impacted the adjuvant effect compared with full Ii-fur. We concluded that the ESS domain is required for full adjuvant efficiency, as this domain is most likely required for reuptake in the endosome and, therefore, further enhancement of MHCII, as indicated by previous results. Because Ii-Cterm-fur produced trimeric Ags, we cannot draw a conclusion on the requirement of trimeric Ag for full adjuvant effect. However, our data suggest that a part of the C-terminal domain of Ii is required for full Ab adjuvant effect, potentially because of its interaction with CD44 and involvement in MIF signaling, as described previously (34, 53). Overall, the results nevertheless indicate that both ESS and the C terminus of Ii were necessary for the full adjuvant effect of the Ii-fur on Ab responses.

Cross-reactivity and inhibition of elicited IgG

To further assess the functionality of the elicited Abs, we tested their capacity to recognize different CIDRα1 protein variants not encoded in the vaccines. Cross-CIDRα1 variant reactivity was

A

1	CIDRa1.1_IT4var19_IT4	10	CIDRa1.2_HB3var1csa_HB3	19	CIDRa1.4_1983-5-1983	28	CIDRa1.6a_PF08_0140_3D7	37	CIDRa1.7_1983-7_1983
2	CIDRa1.1_PFCLINvar30_PFCLIN	11	CIDRa1.3_PFE1640w_3D7	20	CIDRa1.4_1974-5_1974	29	CIDRa1.6a_PFD1235w_3D7	38	CIDRa1.7_2083-1_2083
3	CIDRa1.1_2110-3_2110	12	CIDRa1.4_DD2var32_DD2	21	CIDRa1.5a_1965-2_1965	30	CIDRa1.6b_GA019_ERS010031	39	CIDRa1.8a_1965-3_1965
4	CIDRa1.1_GA011_ERS009959	13	CIDRa1.4_HB3var03_HB3	22	CIDRa1.5a_GA014_ERS010022	31	CIDRa1.6b_GA018_ERS010570	40	CIDRa1.8a_1965-1_1965
5	CIDRa1.1_IGHvar19_IGH	14	CIDRa1.4_IT4var07_IT4	23	CIDRa1.5a_GA013_ERS010323	32	CIDRa1.6b_IT4var18_IT4	41	CIDRa1.8a_GA026_ERS010178
6	CIDRa1.1_IT4var06_IT4	15	CIDRa1.4_PF11_0521_3D7	24	CIDRa1.5b_1918-5_1918	33	CIDRa1.7_1914-14_1914	42	CIDRa1.8a_MAL6P1.316_3D7
7	CIDRa1.1_IT4var20_IT4	16	CIDRa1.4_1918-3_1918	25	CIDRa1.5b_1983-13_1983	34	CIDRa1.7_1965-8_1965	43	CIDRa1.8b_1702-3_1702
8	CIDRa1.1_PFD0020c_3D7	17	CIDRa1.4_GA024_ERS010438	26	CIDRa1.5b_GA017_ERS010601	35	CIDRa1.7_DD2var49_DD2	44	CIDRa1.8b_2053-3_2053
9	CIDRa1.1_RAJ116var08_RAJ116	18	CIDRa1.4 _1994-2_1994	27	CIDRa1.6a_HB3var02_HB3	36	CIDRa1.7_IT4var22_IT4	45	CIDRa1.8b_GA029_ERS010532

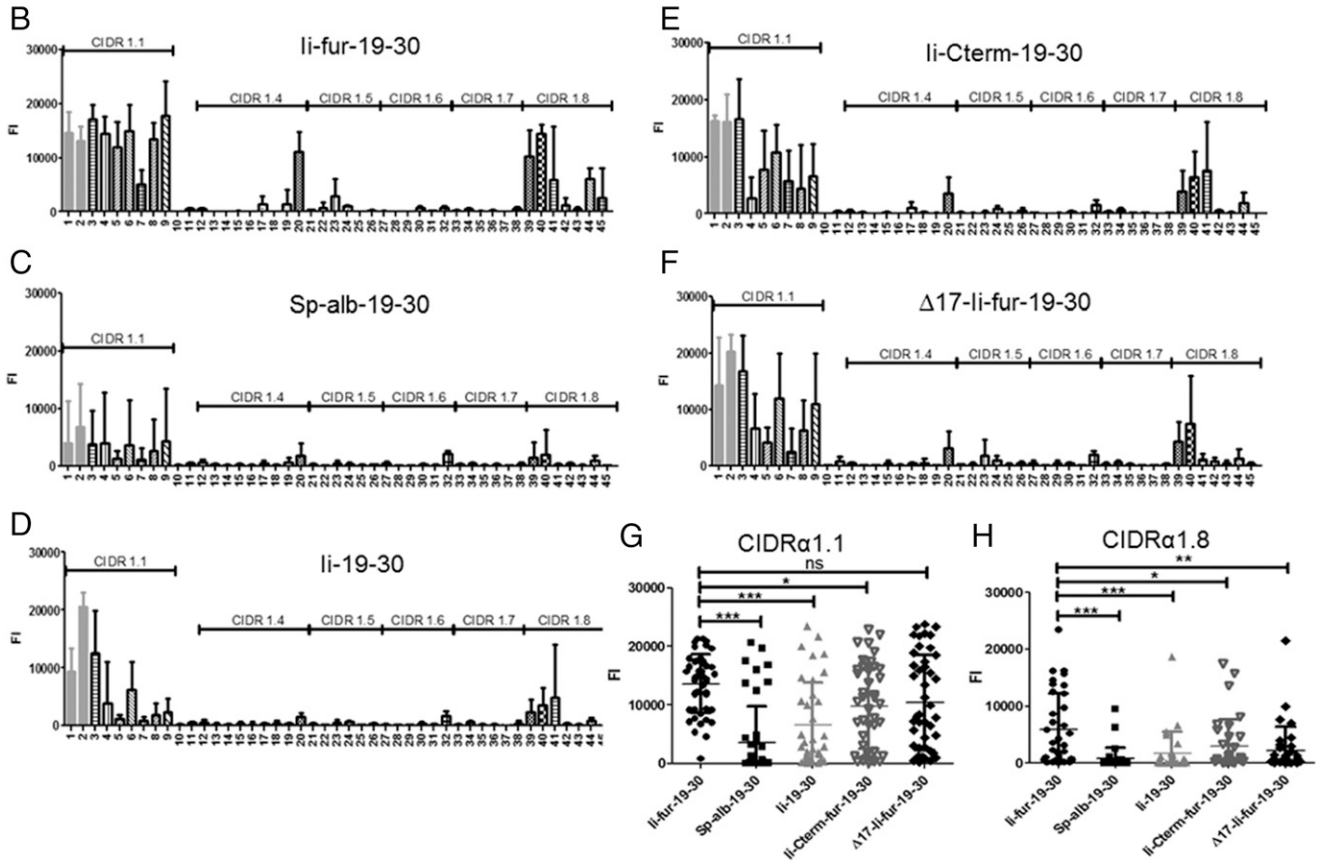

FIGURE 8. Ii-fur adjuvant increases the cross-recognition toward different Ags within the CIDRα1.1 family and with more distant CIDRα1 families. (**A**) Table of the different subtypes of CIDRα1 used for testing the cross-reactivity of the different sera of immunized mice. Each number found on the following bar charts corresponds to one CIDRα1 subtype. (**B**–**F**) Cross-reactive Abs were detected in serum of BALB/c mice 10 wk after vaccination (2 wk after homologous boost) with (B) hAd5–Ii-fur–IT4var19–PFCLINvar30 (n = 5), (C) hAd5–Sp-alb–IT4var19–PFCLINvar30 (n = 5), (D) hAd5–Ii–IT4var19–PFCLINvar30 (n = 4), (E) hAd5–Ii-Cterm-fur–IT4var19–PFCLINvar30 (n = 5), or (F) hAd5–Δ17-Ii-fur–IT4var19–PFCLINvar30 (n = 5) by multiplex. Serum was diluted to 1:50 and incubated with beads coated with different CIDRα1 proteins. Abs binding to the beads were detected by luminescence. (**G** and **H**) All the CIDRα1.1 subtypes (G) or CIDRα1.8 subtypes (H) were grouped and compared between the different immunized groups. Bars represent the mean fluorescence intensity of each group with the SD. Each group was compared with the Ii-fur adjuvant group with nonparametric Mann–Whitney U tests. $*p < 0.05$, $**p < 0.001$, $***p < 0.0001$.

tested in multiplex analysis using a panel of beads, each coated with a different CIDRα1 protein variant and representing all sequence variant types of CIDRα1 (Fig. 8A). For all vaccination experiments, the pattern of cross-reactivity was similar, with cross-reactivity mainly detected between the most closely related sequence types (i.e., CIDRα1.1 and CIDRα1.8 families) (Supplemental Fig. 2). However, the intensity of cross-reactivity was markedly higher with the Ii-fur adjuvant compared with Ii and Sp-alb constructs (Fig. 8B–D), specifically within the families of CIDRα1 domains homologous to the encoded Ags (CIDRα1.1), as we obtained Abs recognizing nine out of nine tested CIDRα1.1 family members, including the two encoded Ags (average [avg.] identity to immunogen, 70%). Additionally, with the Ii-fur adjuvant, five of seven of the most closely related subtype, CIDRα1.8 (avg. identity to immunogen, 49%), were recognized, but there was only detectable reactivity to 2–4 of the remaining 29 more distantly related CIDRα1 variants (avg. identity to immunogen 41%). The data show that cross-reactive Ab responses to CIDRα1 variants were highest in animals who received the Ii-fur adjuvant for the closest relatives, CIDRα1.1 (Fig. 8G) and CIDRα1.8 subtypes (Fig. 8H), and that the presence of the C-terminal part of Ii and ESS domains were also important to obtain cross-reactivity (Fig. 8E, 8F).

For further assessment of the functionality of elicited Abs with the Ii-fur adjuvant, their capacity to inhibit EPCR binding to the encoded IT4var19 and PFLCINvar30 proteins was tested. As EPCR is the natural ligand to the genes encoded in our vaccine, it was important to confirm that the elicited Abs could inhibit the binding of IT4var19 and PFLCINvar30 to EPCR. Compared with Abs elicited by the Ii and Sp-alb constructs, Abs induced after vaccination with Ii-fur exhibited a higher, almost 100% EPCR-binding

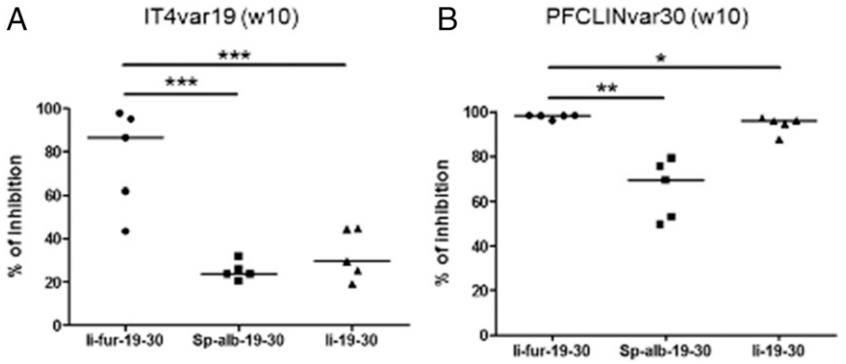

FIGURE 9. Abs induced with Ii-fur adjuvant present a higher capacity to inhibit binding of the encoded malaria Ags to EPCR. (**A**) Detection of Abs inhibiting the binding of CIDRα1.1_IT4var19 to EPCR from week 10 serum after immunization (2 wk after homologous boost) of BALB/c mice with hAd5–Ii-fur–IT4var19–PFCLINvar30 (n = 5), hAd5–Sp-alb–IT4var19–PFCLINvar30 (n = 5), or hAd5–Ii–IT4var19–PFCLINvar30 (n = 5). Serum was diluted to 1:50. (**B**) Detection of Abs inhibiting the binding of CIDRα1.1_PFCLINvar30 to EPCR from week 10 serum after immunization (2 wk after homologous boost) of BALB/c mice with hAd5–Ii-fur–IT4var19–PFCLINvar30 (n = 5), hAd5–Sp-alb–IT4var19–PFCLINvar30 (n = 5), or hAd5–Ii–IT4var19–PFCLINvar30 (n = 5). Serum was diluted to 1:50. Bars represent the median of each group. Each group was compared with the Ii-fur adjuvant group with nonparametric Mann–Whitney U tests. *p <0.05, **$p < 0.001$, ***$p < 0.0001$.

inhibition of the two encoded CIDRα1.1 Ags (Fig. 9). Similar data were observed in the C57BL6 strain of mice (Supplemental Fig. 1). These data suggest that Ii-fur increased the functionality of the Abs either by increasing the quantity (as suggested with the recognition ELISA) or potentially by increasing the quality, too.

Discussion

Recombinant adenoviruses are highly promising delivery vectors for vaccination (54), mostly because they are capable of inducing a high and persistent CD8 T cell response (13) and capable of priming functional Ab responses (17, 55). Among other methods, the MHCII-associated Ii has been shown to be a potent and reliable adjuvant for T cell–mediated immunity after adenoviral vaccination (22, 56, 57). The use of Ii in hAd5 increases and broadens CD8 T cell responses (20, 58) as well as $CD4^+$ T cell responses (59). However, the utility of Ii as an adjuvant for B cell responses is weak (22, 60), and B cell responses are considered essential for most previously successful vaccines.

In this study, we investigated the potential of a secreted version of the Ii adjuvant for inducing B cell responses. The insertion of a fur in the extracellular domain of the Ii was hypothesized to allow Ii-tethered Ag to be secreted in a multimerized form through Ii-mediated trimerization (61). We determined that the tethering of a dimeric Ag to the Ii-fur adjuvant did induce secretion of a trimeric Ii–Ag complex. Unfortunately, the Ii-Cterm-fur mutant, supposed to produce a monomeric form of the Ag, produced a trimeric Ag in a similar ratio to the Ii-fur. Thus, no conclusion on the requirement for a trimeric Ag for the adjuvant effect could be drawn. A complete investigation on the exact conformation of the trimers or the aggregates could not be included in this study; however, our results suggest that Ii-fur induced a better trimeric conformation of the Ag, as shown by higher and specific binding to EPCR, whereas trimeric quantity is similar to Ii-Cterm-fur.

The previously observed T cell adjuvant effect of Ii was preserved after insertion of a fur, and an increase of equivalent MHCI to the surface of the cells was demonstrated. The MHCII presentation of the Ags still retained an adjuvant effect in increased MHCII presentation but was reduced with the furin insertion in comparison with the Ii construct. This was due to the secretion of the Ii–Ag complex and, therefore, the impossibility of reuptake from the surface to the endosomes, as described in previous work (51, 52). However, MHCII presentation disappeared completely after deletion of the ESS domain, emphasizing the role of the ESS for the adjuvant effect, which is necessary for transport to the endosome (for direct or indirect pathway), as predicted from the known function of the ESS domain (31, 52, 62).

Most importantly, the newly designed adjuvant was capable of significantly increasing the Ab response compared with both Ii and a secreted Ag control. This was evident as early as 2 wk post-vaccination and was further enhanced after homologous boost.

The PfEMP1 CIDRα1 proteins constitute a particularly interesting vaccine target, as through evolution, in response to immune selection pressure, the EPCR-binding CIDRα1 domains of PfEMP1 have diversified in sequence but maintained the biochemical and structural requirements for EPCR binding (40). Therefore, by using CIDRα1-based malaria Ags we could investigate the capacity of the Abs to target a broad range of Ag variants needed in most modern vaccines (e.g., influenza, cancer, and malaria). Using the Ii-fur adjuvant, we could show that the Ab response was not only increased to the encoded Ags but also to heterologous CIDRα1 proteins. The breadth of reactivity of elicited Abs to inhibit CIDRα1 variants not included in the vaccination was similar to what was observed in a recent study vaccinating with recombinant CIDRα1 proteins (63).

Furthermore, the increased Ab levels (to both cognate and heterologous CIDRα1 Ags) were shown to be dependent on different parts of the Ii: the secretion through furin insertion, the C-terminal domain, and use of the endosomal pathway. Although our C-terminal construct did not permit a conclusion on the requirement for trimerization of the Ag for full adjuvant effect, we did see that the C-terminal part of the Ii has a role to play in the enhancement of Abs. This can potentially be explained by two different possibilities. 1) The quantification carried out on the protein used in Fig. 4A for binding to EPCR shows that the amount of protein is similar in Ii-fur and Ii-Cterm-fur; however, Ii-Cterm-fur indicated a slightly lower binding to EPCR. This could be due to a lesser amount of correctly conformed Ags and, therefore, less efficiency in inducing structure-dependent Abs. 2) Among various reported functions, the C-terminal part of Ii has been shown to be a coreceptor of CD44, a receptor involved in T cell activation, and could impact MIF signaling (53). This is intriguing, particularly within the scope of malaria, as parasites encode for MIF homologs that inhibit B cell responses (35). This, or indeed a number of other Ii interactions (34) induced by the secreted C-terminal domain, or loss from the cell surface in the vaccine-transduced APCs might therefore explain the difference

seen in adjuvant effect between Ii-fur and Ii-Cterm-fur. With a large number of identified Ii interaction partners (34), mapping such functions goes beyond the scope of this manuscript but would be of interest in future studies and could reveal insights of direct relevance for vaccine design.

In the case of a future malaria vaccine, it is conceivable that further breadth of reactivity and inhibition may be obtained by immunization strategies enhancing rare Ab species, including Abs targeting the structurally conserved EPCR-binding site on CIDRα1 domains, or by immunizing with a panel of Ags covering all EPCR-binding CIDRα1 types. Because of its versatility, the present adenovirus vaccine platform may facilitate both of these scenarios. Nevertheless, the combined T cell and Ab adjuvant effects of Ii-fur–modified adenovirus vaccines may prove useful for targeting other Ags and pathogens, but it will require the ability of the Ii-tethered Ags to fold correctly for induction of conformation-specific Abs. For the work on the CIDRα1 domains, further studies will elucidate if heterologous booster vaccinations can further synergistically enhance the immune responses obtainable after adenoviral vaccination, or if a polyvalent vaccine is a feasible strategy. The outcome of such studies would be relevant for T cell– and Ab-mediated protection alike and be relevant within both malaria and cancer vaccines (17, 64–66).

In summary, we present an analysis of Ab responses induced by the preclinically acclaimed T cell adjuvant Ii (22, 56). We demonstrated that Ii-fur is a further improvement of the adjuvant that can significantly increase MHCI and MHCII Ag presentation as well as Ab responses after adenoviral vaccination. We also showed that several functional parts of the adjuvant converge to jointly increase the immune response to higher levels, including the ESS, the secretion of the Ag via the new fur, and the C-terminal domain attached and secreted with the Ag. Application of this vaccine platform to the polymorphic malaria vaccine candidate, the CIDRα1 PfEMP1 domains, demonstrated the ability to add two diverse Ags in tandem and still elicit a balanced response toward both of them. Thus, albeit that variant transcending responses could not be demonstrated, the Ii-fur–Ag vaccine design may offer new possibilities of achieving broad CIDRα1-variant coverage through further improvements such as heterologous boost, use of different Ag designs, and further exploiting the strategy's potential for increasing polyvalence.

Acknowledgments

We are thankful to Susanne Nielsen, Anne-Marie Andersson, Birita Frittleifsdottir Kjærbæk, and Bang Nguyen for technical assistance. We kindly thank J. Kappler, P. Marrack, and Caroline Benedicte K. Mathiesen for providing us with the BO-97.10 cell line.

Disclosures

P.J.H. has filed for patents relating to immune response priming (European patent application EP15152408.9A, Publication No. EP2865387A2, April 29, 2015, and European patent application EP06818135A, Publication No. WO2007062656A2, June 7, 2007). P.J.H. and C.F. have filed for a patent concerning the development of an improved Ii vaccine adjuvant (European patent application WO2018172259, September 27, 2018). The other authors have no financial conflicts of interest.

References

1. Afkhami, S., Y. Yao, and Z. Xing. 2016. Methods and clinical development of adenovirus-vectored vaccines against mucosal pathogens. *Mol. Ther. Methods Clin. Dev.* 3: 16030.
2. Rollier, C. S., A. Reyes-Sandoval, M. G. Cottingham, K. Ewer, and A. V. Hill. 2011. Viral vectors as vaccine platforms: deployment in sight. *Curr. Opin. Immunol.* 23: 377–382.
3. Deal, C., A. Pekosz, and G. Ketner. 2013. Prospects for oral replicating adenovirus-vectored vaccines. *Vaccine* 31: 3236–3243.
4. Volpers, C., and S. Kochanek. 2004. Adenoviral vectors for gene transfer and therapy. *J. Gene Med.* 6(S1, Suppl. 1): S164–S171.
5. Andre, F. E., R. Booy, H. L. Bock, J. Clemens, S. K. Datta, T. J. John, B. W. Lee, S. Lolekha, H. Peltola, T. A. Ruff, et al. 2008. Vaccination greatly reduces disease, disability, death and inequity worldwide. *Bull. World Health Organ.* 86: 140–146.
6. Xiang, Z. Q., Y. Yang, J. M. Wilson, and H. C. Ertl. 1996. A replication-defective human adenovirus recombinant serves as a highly efficacious vaccine carrier. *Virology* 219: 220–227.
7. He, Z., A. P. Wlazlo, D. W. Kowalczyk, J. Cheng, Z. Q. Xiang, W. Giles-Davis, and H. C. Ertl. 2000. Viral recombinant vaccines to the E6 and E7 antigens of HPV-16. *Virology* 270: 146–161.
8. Choi, Y., and J. Chang. 2013. Viral vectors for vaccine applications. *Clin. Exp. Vaccine Res.* 2: 97–105.
9. Ahi, Y. S., D. S. Bangari, and S. K. Mittal. 2011. Adenoviral vector immunity: its implications and circumvention strategies. *Curr. Gene Ther.* 11: 307–320.
10. Yang, T. C., K. Dayball, Y. H. Wan, and J. Bramson. 2003. Detailed analysis of the CD8+ T-cell response following adenovirus vaccination. *J. Virol.* 77: 13407–13411.
11. Lambert, P. H., M. Liu, and C. A. Siegrist. 2005. Can successful vaccines teach us how to induce efficient protective immune responses? *Nat. Med.* 11 (4, Suppl.): S54–S62.
12. Yang, T. C., J. B. Millar, N. Grinshtein, J. Bassett, J. Finn, and J. L. Bramson. 2007. T-cell immunity generated by recombinant adenovirus vaccines. *Expert Rev. Vaccines* 6: 347–356.
13. Bassett, J. D., S. L. Swift, and J. L. Bramson. 2011. Optimizing vaccine-induced CD8(+) T-cell immunity: focus on recombinant adenovirus vectors. *Expert Rev. Vaccines* 10: 1307–1319.
14. Chaudhri, G., V. Tahiliani, P. Eldi, and G. Karupiah. 2015. Vaccine-induced protection against orthopoxvirus infection is mediated through the combined functions of CD4 T cell-dependent antibody and CD8 T cell responses. *J. Virol.* 89: 1889–1899.
15. Spensieri, F., E. Siena, E. Borgogni, L. Zedda, R. Cantisani, N. Chiappini, F. Schiavetti, D. Rosa, F. Castellino, E. Montomoli, et al. 2016. Early rise of blood T follicular helper cell subsets and baseline immunity as predictors of persisting late functional antibody responses to vaccination in humans. *PLoS One* 11: e0157066.
16. Sette, A., M. Moutaftsi, J. Moyron-Quiroz, M. M. McCausland, D. H. Davies, R. J. Johnston, B. Peters, M. Rafii-El-Idrissi Benhnia, J. Hoffmann, H. P. Su, et al. 2008. Selective CD4+ T cell help for antibody responses to a large viral pathogen: deterministic linkage of specificities. *Immunity* 28: 847–858.
17. Andersson, A. C., M. Resende, A. Salanti, M. A. Nielsen, and P. J. Holst. 2017. Novel adenovirus encoded virus-like particles displaying the placental malaria associated VAR2CSA antigen. *Vaccine* 35: 1140–1147.
18. Li, Y., D. B. Leneghan, K. Miura, D. Nikolaeva, I. J. Brian, M. D. Dicks, A. J. Fyfe, S. E. Zakutansky, S. de Cassan, C. A. Long, et al. 2016. Enhancing immunogenicity and transmission-blocking activity of malaria vaccines by fusing Pfs25 to IMX313 multimerization technology. *Sci. Rep.* 6: 18848.
19. Xu, Z. L., H. Mizuguchi, A. Ishii-Watabe, E. Uchida, T. Mayumi, and T. Hayakawa. 2002. Strength evaluation of transcriptional regulatory elements for transgene expression by adenovirus vector. *J. Control. Release* 81: 155–163.
20. Holst, P. J., M. R. Sorensen, C. M. Mandrup Jensen, C. Orskov, A. R. Thomsen, and J. P. Christensen. 2008. MHC class II-associated invariant chain linkage of antigen dramatically improves cell-mediated immunity induced by adenovirus vaccines. *J. Immunol.* 180: 3339–3346.
21. Diebold, S. S., M. Cotten, N. Koch, and M. Zenke. 2001. MHC class II presentation of endogenously expressed antigens by transfected dendritic cells. *Gene Ther.* 8: 487–493.
22. Spencer, A. J., M. G. Cottingham, J. A. Jenks, R. J. Longley, S. Capone, S. Colloca, A. Folgori, R. Cortese, A. Nicosia, M. Bregu, and A. V. Hill. 2014. Enhanced vaccine-induced CD8+ T cell responses to malaria antigen ME-TRAP by fusion to MHC class ii invariant chain. *PLoS One* 9: e100538.
23. Xu, H., A. M. Andersson, E. Ragonnaud, D. Boilesen, A. Tolver, B. A. H. Jensen, J. L. Blanchard, A. Nicosia, A. Folgori, S. Colloca, et al. 2017. Mucosal vaccination with heterologous viral vectored vaccine targeting subdominant SIV accessory antigens strongly inhibits early viral replication. *EBioMedicine* 18: 204–215.
24. Paz, P., N. Brouwenstijn, R. Perry, and N. Shastri. 1999. Discrete proteolytic intermediates in the MHC class I antigen processing pathway and MHC I-dependent peptide trimming in the ER. *Immunity* 11: 241–251.
25. Chikhlikar, P., L. Barros de Arruda, M. Maciel, P. Silvera, M. G. Lewis, J. T. August, and E. T. Marques. 2006. DNA encoding an HIV-1 Gag/human lysosome-associated membrane protein-1 chimera elicits a broad cellular and humoral immune response in Rhesus macaques. *PLoS One* 1: e135.
26. de Arruda, L. B., P. R. Chikhlikar, J. T. August, and E. T. Marques. 2004. DNA vaccine encoding human immunodeficiency virus-1 Gag, targeted to the major histocompatibility complex II compartment by lysosomal-associated membrane protein, elicits enhanced long-term memory response. *Immunology* 112: 126–133.
27. Wu, T. C., F. G. Guarnieri, K. F. Staveley-O'Carroll, R. P. Viscidi, H. I. Levitsky, L. Hedrick, K. R. Cho, J. T. August, and D. M. Pardoll. 1995. Engineering an intracellular pathway for major histocompatibility complex class II presentation of antigens. *Proc. Natl. Acad. Sci. USA* 92: 11671–11675.
28. Parra-López, C. A., R. Lindner, I. Vidavsky, M. Gross, and E. R. Unanue. 1997. Presentation on class II MHC molecules of endogenous lysozyme targeted to the endocytic pathway. *J. Immunol.* 158: 2670–2679.
29. Bakke, O., and B. Dobberstein. 1990. MHC class II-associated invariant chain contains a sorting signal for endosomal compartments. *Cell* 63: 707–716.

30. Lotteau, V., L. Teyton, A. Peleraux, T. Nilsson, L. Karlsson, S. L. Schmid, V. Quaranta, and P. A. Peterson. 1990. Intracellular transport of class II MHC molecules directed by invariant chain. *Nature* 348: 600–605.
31. Pieters, J., O. Bakke, and B. Dobberstein. 1993. The MHC class II-associated invariant chain contains two endosomal targeting signals within its cytoplasmic tail. *J. Cell Sci.* 106: 831–846.
32. Odorizzi, C. G., I. S. Trowbridge, L. Xue, C. R. Hopkins, C. D. Davis, and J. F. Collawn. 1994. Sorting signals in the MHC class II invariant chain cytoplasmic tail and transmembrane region determine trafficking to an endocytic processing compartment. *J. Cell Biol.* 126: 317–330.
33. Cresswell, P. 1996. Invariant chain structure and MHC class II function. *Cell* 84: 505–507.
34. Schröder, B. 2016. The multifaceted roles of the invariant chain CD74--more than just a chaperone. *Biochim. Biophys. Acta* 1863(6, 6 Pt A): 1269–1281.
35. Baeza Garcia, A., E. Siu, T. Sun, V. Exler, L. Brito, A. Hekele, G. Otten, K. Augustijn, C. J. Janse, J. B. Ulmer, et al. 2018. Neutralization of the *Plasmodium*-encoded MIF ortholog confers protective immunity against malaria infection. *Nat. Commun.* 9: 2714.
36. Thomas, G. 2002. Furin at the cutting edge: from protein traffic to embryogenesis and disease. *Nat. Rev. Mol. Cell Biol.* 3: 753–766.
37. Gonçalves, B. P., C. Y. Huang, R. Morrison, S. Holte, E. Kabyemela, D. R. Prevots, M. Fried, and P. E. Duffy. 2014. Parasite burden and severity of malaria in Tanzanian children. *N. Engl. J. Med.* 370: 1799–1808.
38. Turner, L., T. Lavstsen, S. S. Berger, C. W. Wang, J. E. Petersen, M. Avril, A. J. Brazier, J. Freeth, J. S. Jespersen, M. A. Nielsen, et al. 2013. Severe malaria is associated with parasite binding to endothelial protein C receptor. *Nature* 498: 502–505.
39. Jespersen, J. S., C. W. Wang, S. I. Mkumbaye, D. T. Minja, B. Petersen, L. Turner, J. E. Petersen, J. P. Lusingu, T. G. Theander, and T. Lavstsen. 2016. Plasmodium falciparum var genes expressed in children with severe malaria encode CIDRα1 domains. *EMBO Mol. Med.* 8: 839–850.
40. Lau, C. K., L. Turner, J. S. Jespersen, E. D. Lowe, B. Petersen, C. W. Wang, J. E. Petersen, J. Lusingu, T. G. Theander, T. Lavstsen, and M. K. Higgins. 2015. Structural conservation despite huge sequence diversity allows EPCR binding by the PfEMP1 family implicated in severe childhood malaria. *Cell Host Microbe* 17: 118–129.
41. Holst, P. J., C. Bartholdy, A. Stryhn, A. R. Thomsen, and J. P. Christensen. 2007. Rapid and sustained CD4(+) T-cell-independent immunity from adenovirus-encoded vaccine antigens. *J. Gen. Virol.* 88: 1708–1716.
42. Chartier, C., E. Degryse, M. Gantzer, A. Dieterle, A. Pavirani, and M. Mehtali. 1996. Efficient generation of recombinant adenovirus vectors by homologous recombination in *Escherichia coli*. *J. Virol.* 70: 4805–4810.
43. Cottingham, M. G., F. Carroll, S. J. Morris, A. V. Turner, A. M. Vaughan, M. C. Kapulu, S. Colloca, L. Siani, S. C. Gilbert, and A. V. Hill. 2012. Preventing spontaneous genetic rearrangements in the transgene cassettes of adenovirus vectors. *Biotechnol. Bioeng.* 109: 719–728.
44. Becker, T. C., R. J. Noel, W. S. Coats, A. M. Gómez-Foix, T. Alam, R. D. Gerard, and C. B. Newgard. 1994. Use of recombinant adenovirus for metabolic engineering of mammalian cells. *Methods Cell. Biol.* 43 Pt A: 161–189.
45. Cham, G. K., J. Kurtis, J. Lusingu, T. G. Theander, A. T. Jensen, and L. Turner. 2008. A semi-automated multiplex high-throughput assay for measuring IgG antibodies against *Plasmodium falciparum* erythrocyte membrane protein 1 (PfEMP1) domains in small volumes of plasma. *Malar. J.* 7: 108.
46. Hugo, P., J. W. Kappler, J. E. McCormack, and P. Marrack. 1993. Fibroblasts can induce thymocyte positive selection in vivo. *Proc. Natl. Acad. Sci. USA* 90: 10335–10339.
47. Ragonnaud, E., A. M. Andersson, A. E. Pedersen, H. Laursen, and P. J. Holst. 2016. An adenoviral cancer vaccine co-encoding a tumor associated antigen together with secreted 4-1BBL leads to delayed tumor progression. *Vaccine* 34: 2147–2156.
48. Jensen, A. T., A. Ismail, A. Gaafar, A. M. El Hassan, and T. G. Theander. 2002. Humoral and cellular immune responses to glucose regulated protein 78–a novel *Leishmania donovani* antigen. *Trop. Med. Int. Health* 7: 471–476.
49. Holst, P., A. Thomsen, J. Christensen, and M. Grujic, inventors; Kobenhavns Universitet, assignee. Priming of an immune response. European patent application EP15152408.9A, Publication No. EP2865387A2. 2015 April 29.
50. Madsen, C. B., C. Petersen, K. Lavrsen, M. Harndahl, S. Buus, H. Clausen, A. E. Pedersen, and H. H. Wandall. 2012. Cancer associated aberrant protein O-glycosylation can modify antigen processing and immune response. *PLoS One* 7: e50139.
51. Gupta, S. N., M. M. Kloster, D. G. Rodionov, and O. Bakke. 2006. Re-routing of the invariant chain to the direct sorting pathway by introduction of an AP3-binding motif from LIMP II. *Eur. J. Cell Biol.* 85: 457–467.
52. Hofmann, M. W., S. Höning, D. Rodionov, B. Dobberstein, K. von Figura, and O. Bakke. 1999. The leucine-based sorting motifs in the cytoplasmic domain of the invariant chain are recognized by the clathrin adaptors AP1 and AP2 and their medium chains. *J. Biol. Chem.* 274: 36153–36158.
53. Leng, L., C. N. Metz, Y. Fang, J. Xu, S. Donnelly, J. Baugh, T. Delohery, Y. Chen, R. A. Mitchell, and R. Bucala. 2003. MIF signal transduction initiated by binding to CD74. *J. Exp. Med.* 197: 1467–1476.
54. Lasaro, M. O., and H. C. Ertl. 2009. New insights on adenovirus as vaccine vectors. *Mol. Ther.* 17: 1333–1339.
55. Barouch, D. H., G. Alter, T. Broge, C. Linde, M. E. Ackerman, E. P. Brown, E. N. Borducchi, K. M. Smith, J. P. Nkolola, J. Liu, et al. 2015. Protective efficacy of adenovirus/protein vaccines against SIV challenges in rhesus monkeys. *Science* 349: 320–324.
56. Capone, S., M. Naddeo, A. M. D'Alise, A. Abbate, F. Grazioli, A. Del Gaudio, M. Del Sorbo, M. L. Esposito, V. Ammendola, G. Perretta, et al. 2014. Fusion of HCV nonstructural antigen to MHC class II-associated invariant chain enhances T-cell responses induced by vectored vaccines in nonhuman primates. *Mol. Ther.* 22: 1039–1047.
57. Mikkelsen, M., P. J. Holst, J. Bukh, A. R. Thomsen, and J. P. Christensen. 2011. Enhanced and sustained CD8+ T cell responses with an adenoviral vector-based hepatitis C virus vaccine encoding NS3 linked to the MHC class II chaperone protein invariant chain. *J. Immunol.* 186: 2355–2364.
58. Grujic, M., P. J. Holst, J. P. Christensen, and A. R. Thomsen. 2009. Fusion of a viral antigen to invariant chain leads to augmented T-cell immunity and improved protection in gene-gun DNA-vaccinated mice. *J. Gen. Virol.* 90: 414–422.
59. Rowe, H. M., L. Lopes, Y. Ikeda, R. Bailey, I. Barde, M. Zenke, B. M. Chain, and M. K. Collins. 2006. Immunization with a lentiviral vector stimulates both CD4 and CD8 T cell responses to an ovalbumin transgene. *Mol. Ther.* 13: 310–319.
60. Holst, P. J., A. R. Thomsen, and J. P. Christensen, inventors; Kobenhavns Universitet, assignee. A nucleotide vaccine. European patent application EP06818135A, Publication No. WO2007062656A2. 2007 June 7.
61. Ashman, J. B., and J. Miller. 1999. A role for the transmembrane domain in the trimerization of the MHC class II-associated invariant chain. *J. Immunol.* 163: 2704–2712.
62. Bremnes, B., T. Madsen, M. Gedde-Dahl, and O. Bakke. 1994. An LI and ML motif in the cytoplasmic tail of the MHC-associated invariant chain mediate rapid internalization. *J. Cell Sci.* 107: 2021–2032.
63. Turner, L., T. G. Theander, and T. Lavstsen. 2018. Immunization with recombinant plasmodium falciparum erythrocyte membrane protein 1 CIDRα1 domains induces domain subtype inhibitory antibodies. *Infect. Immun.* 86: e00435-18.
64. Tatsis, N., S. W. Lin, K. Harris-McCoy, D. A. Garber, M. B. Feinberg, and H. C. Ertl. 2007. Multiple immunizations with adenovirus and MVA vectors improve CD8+ T cell functionality and mucosal homing. *Virology* 367: 156–167.
65. Reyes-Sandoval, A., T. Berthoud, N. Alder, L. Siani, S. C. Gilbert, A. Nicosia, S. Colloca, R. Cortese, and A. V. Hill. 2010. Prime-boost immunization with adenoviral and modified vaccinia virus Ankara vectors enhances the durability and polyfunctionality of protective malaria CD8+ T-cell responses. *Infect. Immun.* 78: 145–153.
66. Patterson, L. J., and M. Robert-Guroff. 2008. Replicating adenovirus vector prime/protein boost strategies for HIV vaccine development. *Expert Opin. Biol. Ther.* 8: 1347–1363.